2011

The Characterization of Genes Involved in Response to the Phenol Derivative and Xenoestrogen Bisphenol-A in Saccharomyces Cerevisiae

Sasha N. Farina
Claremont Mckenna College

`

The characterization of genes involved in response to the phenol derivative and xenoestrogen bisphenol-A in *Saccharomyces cerevisiae:*

implication of the high osmolarity glycerol pathway as a first line of defense.

By

Sasha Farina

Thesis Advisor: Dr. Gretchen Edwalds-Gilbert

Senior Thesis in Biology

Claremont Mckenna College

25th of April, 2011

Table of Contents

I. Abstract

Bisphenol A is an estrogenic compound that is found in polycarbonate plastics and epoxy resins; humans are continuously exposed to the compound and it is believed to possess the same carcinogenic effects as estrogen (Iso, 2006). In this study, I used *Saccharomyces cerevisiae* as a model organism to identify mechanisms by which BPA acts based on the genomic profiling of kinase genes from a Mat-α haploid deletion library. Kinases regulate many other proteins, so the identification of a single mutant could identify an entire affected pathway of genes. I conducted a systematic screen of these mutants using the phenotype of growth inhibition. Using solid growth assays, I identified 17 BPA sensitive mutants, six of which were related to the high osmolarity growth pathway, which is involved in osmotic stress response and could be a mechanism of defense of *S. cerevisiae* against BPA. I implemented liquid growth assays, protein analysis, as well as microscopy for a more in depth study of the effects of BPA on these mutants. Bisphenol-A initially inhibits the growth of *S. cerevisiae*, however, there were some strains that appeared to show adaptation in the presence of the compound. I found that BPA inhibits cell cycle progression, and may affect the phosphorylation regulation of Cdc28, but without affecting the production of the protein. This study could provide clues for predicting the effects of BPA on homologous genes in mammals and identifying similar pathways of resistance. By having a better understanding of the effects on BPA on the cell, the compound can be better regulated by the EPA and complications resulting from continuous exposure to BPA can be treated effectively.

II. Introduction

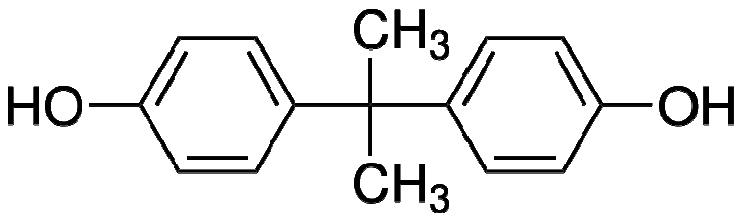

Figure 1. Chemical Structure of bisphenol A (http://rheothing.blogspot.com/2010/09/bpa.html)

Humans are constantly exposed to many environmental substances that exhibit activity that alters the endocrine system (Walsh, 2005). Bisphenol A is a very stable compound that can be found in polycarbonate plastics and epoxy resins (Fig 1). Polycarbonate plastics and epoxy resins are used in a number of things, such as impact-resistant safety equipment, baby bottles, protective coatings inside metal food containers, and sealants in dentistry (Calafat, 2008). BPA was found to be leaching out of polycarbonate flasks when scientists were conducting a study on the estrogenic activity of *S. cerevisiae* (Krishnan, 1993). This finding caused uproar in the world of environmental science, because it suggested that BPA is able to leach out of products that we use every day. The study also found that the compound has a 1:2000 potency ratio compared to estradiol (Krishnan, 1993). Although this ratio appears to be weak, the continuous exposure of humans to BPA could increase its ability to cause estrogenic effects on the human body. Since the discovery of leaching BPA, it has been the focus of several studies through the years.

It is believed that people are exposed to BPA from the ingestion of food, which can leach into it from plastic linings in storage containers such as cans (Calafat, 2008). Almost

everybody is exposed to BPA in some way, shape, or form: it has been found that BPA is present in the urine of about 92.6% of people above the age of 6 (Calafat, 2008).

It has been found that BPA has exhibited estrogen-like effects on uterine and prostate organ weights in experiment animals (Calafat, 2008). There have also been reports of BPA causing decreased sperm production, prostate gland volume, deficiency in mammary gland development, abnormal vaginal morphology, and interruption of sexual differentiation in the brain as well as accelerated growth and earlier onset of puberty (Calafat, 2008). More so, it is believed to mimic estrogen by exhibiting carcinogenic effects through its genotoxicity, and its ability to stimulate cell proliferation (Iso, 2006). Estrogen can cause DNA damage from its estrogen-like metabolites, derived oxidants, and the formation of micronuclei; it has been found that BPA acts similarly as 17β-estradiol to cause DNA damage (Iso, 2006).

Studies have shown that BPA has an estimated half life of 6 hours in humans, which suggests that humans are continuously exposed to it (Calafat, 2008). The lipophilic properties of BPA are what may cause it to be so dangerous, and also cause estimations of exposure to be very inaccurate. Although estimations of exposure to BPA is only within micromoles ($1x10^7$) (Wetherill, 2007), accumulation in fat and tissues can cause it to reach much higher and more dangerous concentrations within the body (Walsh, 2005). The phenol can be released into the blood during lypolysis at much greater concentrations than the original exposure (Hughes, 2000). Take for example, the implication that exposure to BPA can cause breast cancer (Walsh, 2005), breasts are composed of fatty tissues and thus can be at greater risk to carcinogenic effects of BPA than other tissues. Despite the numerous studies on this compound, most tend to focus on the estrogenic activities of BPA and not on other possible mechanisms.

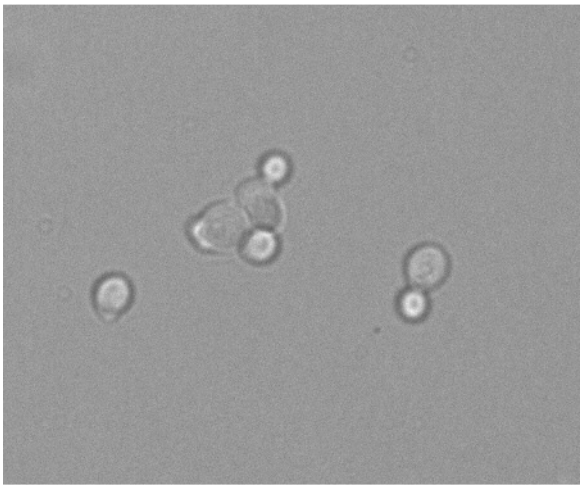

Figure 2. ***Saccharomyces cerevisiae.*** Bright field image of wild type yeast at 60x.

Overall, there is a serious lack of studies that seek alternative ways that BPA acts on the cell. While most of the scientific community agrees that BPA exhibits estrogenic effects, it is still unclear what other ways BPA could be affecting a cell. There is great disparity between how potent the compound is and its binding affinity to estrogen-like receptors, which would imply that there are several other mechanisms it uses (Kirk, 2003). Wetherill et al. 2007 state that "the lack of an integrated and systemic understanding of BPA's endocrine disruptive actions has considerably complicated risk assessment efforts and safety recommendations by regulatory agencies." It is important to identify these other mechanisms that BPA acts in order to adequately treat exposure.

Saccharomyces cerevisiae is a model organism that has been used for numerous genomic screen studies (Fig 2). Budding yeast has ~6,000 genes, many of which are homologs to humans and other organisms. Greater than 40% of yeast proteins contain conserved sequences with at least one known or predicted human protein (Baetz, 2004). *S. cerevisiae* is generally easy to work with, and because of this, the organism is used as a

preliminary model to more advanced studies on complex organisms, such as mammalian cells. The entire genome of *S. cerevisiae* has been systematically deleted of its genes to develop genomic libraries.

Genomic libraries of *S. cerevisiae* have been used to "identify the targets underlying their therapeutic action and unwanted effects" of drugs and other compounds (Baetz, 2004). This process is known as genomic screening, in which yeast mutants with single genes knocked out of them are tested for sensitivity to various compounds. The sensitivity or resistance of a specific mutant can either imply that the gene is a target of the compound, or that the gene is involved in some form of defense mechanism to the compound. Chemicals that can be characterized through phenotypic genomic screens "are valuable chemical genetic tools to study complex cellular processes and are often attractive candidates for drug development" (Baetz, 2004). Genome screening is efficient because there is often no prior knowledge of the pathways affected by drugs, so the typical guess and check approach is not very successful (Baetz, 2004). The classical approach of drug target screening is to purify possible targets from cellular extracts, and test them one by one systematically through binding assays or functional assays, such as modifying active regions of a protein to see if the function is lost (Baetz, 2004). This sort of method is tedious and time consuming, and presently genomic screens have been the norm. This study applies the genomic screen approach to a Mat-α haploid kinase deletion library to observe the effects of BPA on kinase pathways in *S. cerevisiae.*

Protein kinases are one of the largest carriers of information within the cell other than nucleic acids. They are enzymes that can be activated or deactivated by using cell surface or internal receptors and respond via kinase cascades to provide possibly the most interrelated

network of macromolecules in cells (Levy, 2010). The classical view of kinase interaction is the "textbook depicted linear cascade", which is good for understanding specific branches and regions, but is not useful for understanding the big picture of a kinase interaction network (Levy, 2010). The cascade model of kinase interaction suggests that the kinase network, although muddled and complex, could be one of the most precisely regulated networks in the cell. Deactivating or activating a single kinase could be responsible for shutting down entire pathways, not to mention there are several kinases that participate in more than one pathway.

It isn't very well understood how these kinases are regulated so well and has been a focus of many recent studies. Breitkrutz found that ~30% of interactions among kinases are what would not be expected by chance, which implies that there are large amounts of cross talk between pathways (Breitkrutz, 2010). Kinases can phosphorylate other kinases as well as activate or deactivate proteins that are involved in gene transcription. Studies have shown that kinases are more highly phosphorylated than other proteins; the inhibition of a kinase results in the decreased or increased phosphorylation of proteins (Levy, 2010). Levy suggests that the kinase-phosphatase interaction network is similar to transcriptional regulatory networks.

Apart from genetic analyses, *S. cerevisiae* is used as a model system to study the cell cycle because it is very similar to eukaryotic cells except for the absence of a nuclear envelope and the fact that daughter cells emerge through budding rather than the splitting of the cell (Niu, 2008). Analysis of the cell cycle can give insight on where and when genetic defects may be occurring and can point in the right direction towards a mechanism of a drug

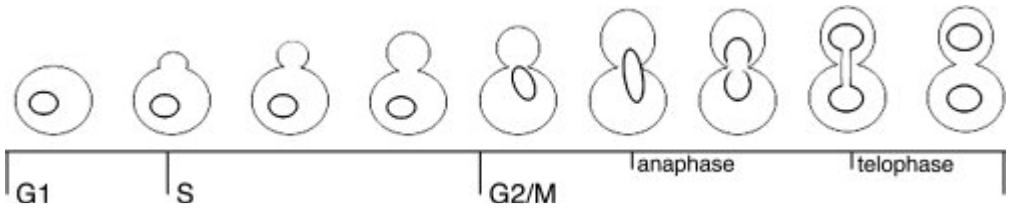

Figure 3. ***S. cerevisiae*** **cell cycle** (Calvert, 2008). This figure depicts the cell cycle of *S. cerevisiae*; it is important to note the location of the nuclei, as it is an important indicator of the cell cycle stage that the cell is in. This model formed the basis of my cell cycle observations.

action (Niu, 2008). There are four major cell cycle phases: 1. (G1) growth gap phase, 2. (S) DNA synthesis, 3. (G2) second growth gap phase, and 4. (M) mitotic cell division (see Figure 3). It is the distribution in which the cells are in each phase that can tell us whether the cell cycle is disrupted in a particular strain. In this study, I used fluorescence microscopy with DAPI staining to determine the cell cycle phases.

This study seeks to identify possible mechanisms by which BPA acts on the cell based on genomic profiling of kinase genes in *Saccharomyces cerevisiae*. Because kinases regulate many other proteins, the identification of a single mutant may provide insight on the interaction of the entire pathway with BPA. We have used phenotypic profiling to narrow down and identify these targets, via cell growth assays, microscopy, and protein analysis.

III. Materials and Methods

Library maintenance and screening: Extreme sterility was used during these procedures. All steps were performed in a tissue culture hood that had been UV sterilized at least 30 min. After UV sterilization of the hood and tools to be used for the library, every surface of the hood and the tools were wiped down with EtOH, and the blower was kept on whenever the hood was open. The master copies of the haploid mat-α deletion library (Open Biosystems) were stored at -80°C and thawed inside the hood when they were to be used. For replication of the master library, 96 well plates were used. 150 µl of a mixture of YPD and G418 (200 ug/mL) was added to each well. The plates were incubated at 30°C overnight to ensure that there was no contamination. The plates were then inoculated using a sterile replicator (Genetix) to transfer cells from the master plates to the working copies. The plates were incubated at least 48 hours at 30°C to allow the cells to grow. Before storing at -80°C, a mixture of 32% DMSO and H_2O was added to each well to give a final concentration of 8% DMSO as well as glycerol for a final concentration of 15%. The DMSO is needed so that the water does not crystallize and break open the cells when frozen at such low temperatures. The strains used to create the kinase deletion working plates were transferred using 5 µl of inoculate and transferring to a new plate, prepared in the procedure described above.

Colony growth assay: Synthetic defined (SD, Sunrise Biosciences) media with agar were used for these screens. Stock solutions of BPA (Sigma) were created by adding 1 mL 100% DMSO to 0.079 g of BPA for a final concentration of 350 mM BPA. The stock of BPA and DMSO were filter sterilized and were used within 5 days of creating the stock

solution. Approximately 100 µl of BPA or 100 µl DMSO control were added to the agar for a final concentration of 1 mM BPA. The agar was put in a 60°C water bath *immediately* after coming out of the autoclave to preserve its ability to dissolve the compounds. Each plate was then created, one at a time, in 50 mL conical tubes by adding 35 mL of SD agar and 100 µl of stock solution, inverting gently, and then pouring into a plate, without bubbles. The plates were then allowed to dry overnight, and spotted the next day inside a hood to maintain sterility. About 7 µl of cells was optimal for spotting onto SD agar. Once the plates were dry, they were incubated at 30°C for about 48 hours. The plates were then scanned with an HP scanner in grayscale as a record of the results, but the actual observations were always analyzed from the plate itself.

Spot dilution assays: The 180 strain kinase and DNA repair deletion library was narrowed down to 18 strains including the wild type, based on the frequency and consistency of sensitivity of each strain to its control strain. Overnight inoculates were grown in 3 mL cultures overnight in SD media without BPA. The OD_{600} for the strains was measured and they were diluted so that the starting cell concentration would be the same for all strains. The dilutions were set up in a 96 well plate, starting with 180 µl of $6x10^6$ cells/mL, and then serially diluting by factors of 10 to a final concentration of $6x10^1$ cells/mL. SD agar was used for this assay with the technique mentioned in the colony growth assay, and 7 µl of cells were spotted onto plates containing either 1 mM BPA or 100% DMSO. The plates were then allowed to grow for at least 4 days at 30°C. The plates were all scanned for recording purposes, but the observations were taken from the actual plate.

Growth Curves: According to the procedure by Baetz et al. 2004, overnight inoculates were grown in 3 mL of SD media without BPA. The OD_{600} was measured and the strains were diluted to approximately $3x10^5$ cells/mL in 10 mL of SD media without BPA in it. All experiments were performed in triplicate. The cells were then allowed to grow for approximately 2.5-3 hours and the OD_{600} was measured again. Ideally, one should wait till the cells reach an OD_{600} of 0.05, but due to time constraints and differences in the growth rates of strains, this was not the case in my study. The cells reached an OD_{600} of about 0.02-0.04 and then BPA or DMSO was added to the culture to a final concentration of 0.8 mM BPA. It is more important that the control and experimental mutant have similar concentrations rather than with the whole group itself (i.e. Δmck1 plus BPA and Δmck1 plus DMSO should have similar values, but in general grow much slower than the other deletion strains). The time when the compound is added is time=0 and time points are taken across 10 hours (ideally once every hour). Not every strain of the 17 were used in this assay. They were chosen based on their relevance to the high osmolarity glycerol pathway in *S. cerevisiae.*

Inhibitory Concentration Calculations: The method using growth curves described above was utilized to determine the inhibitory concentration with 50% survivial (IC-50), using wild type strain and 0.4, 0.6 and 0.8 mM BPA. From the final OD_{600} the percent survival of cells was plotted, percent survival vs. [BPA], with the WT +DMSO serving as 100% growth and dividing the other concentrations by that number. The linear trend line generated from the data was used to calculate the IC-50 of wild type *S. cerevisiae* in liquid SD media.

DAPI staining and Fluorescence Microscopy: Cells were inoculated overnight in SD media, and then grown in the same manner as the growth curves for exposure to BPA. They were allowed to grow in 10 mL of SD media before adding the compound. They were grown until more than $1x10^7$ cells could be harvested from the culture. $1x10^7$ cells were centrifuged and washed with sterile water before resuspending the cell pellet in 1 mL of cold 70% EtOH. 100 µl of the resuspension was aliquoted to a new tube and washed again with 1 mL sterile water. The pellet was resuspended in 100 µl sterile water. 5 µl of the suspension was added to a microscope slide, and when dried, one drop of DAPI (Prolong Gold Antifade Reagent, Invitrogen) reagent was added (with protection from light!) and incubated for 24 hours. The cells were visualized using a Nikon camera microscope and NCIX software and analyzed with bright field in conjunction with the filter that is appropriate for visualizing DAPI. Around 10-12 sets of pictures were taken of each field of view: bright field, DAPI, and dual, ensuring that there were more than 10 cells in each picture so that the final cell analysis count was not below 100 cells.

Protein extraction: Overnight inoculates were diluted to approximately $3x10^5$ cells/mL in 50 mL of SD media. The OD_{600} was measured until the cells reached an OD_{600} of 0.05, at which point the BPA/DMSO was added to a final concentration of 0.8mM (adjusting for the amount of media gone from taking density measurements). The cells were then allowed to grow until they reached a density that allowed for the harvesting of $1x10^9$ cells. All of the subsequent steps were performed at 4°C whenever possible. The strains were centrifuged at 15,000 x g for 5 min. The cells were then washed in 2 mL of sterile water and centrifuged again at 15,000 x g for 5 min. The cell pellet was stored at 4°C. When ready for

extraction, the pellet was resuspended in 500 µl glass beads (Sigma) and in 500 mL buffer A containing protease inhibitor, adding 10 µl Halt Protease Inhibitor (Thermo Scientific) for every 1 mL of cold buffer A (10 mM HEPES pH 7.8, 1.5 mM $MgCl_2$, 10 µM KCl, 0.5 mM DTT) needed. The cells were broken via vortexing with 5 cycles of a 30 sec. vortex burst followed by 30 sec. rest on ice. The samples were centrifuged at 10,000 x g for 5 min. and 400 µl of supernatant was transferred to a new tube containing 40 µl of cold 2M KCl. The solution was mixed and incubated on ice for 5 min, then centrifuged at top speed (13,000 x g) for 20 min. The supernatant was transferred to new tubes and stored at -20°C. Due to trouble interpreting results from the western blot, the protein concentration was verified via Bradford assay, they were all relatively the same.

SDS-Page and Western Blotting: Approximately 9 µl of sample was added with 3 µl of 4X protein dye reagent and incubated at 70°C for 5 min. The gels (4-15% Mini Protean®TGX™, BioRad) were set up by adding SDS-Page buffer (1% SDS, 2.5 M glycine, 30.2 g Tris Base, in 1 L H_2O) inside the gel dam and removing the comb carefully, in the BioRad Mini Trans-blot. It is important to pipet up and down in the wells to ensure they are good. Samples were then loaded onto protean gels and ran at 200 volts for about 45 min or however long it takes for the dye front to reach the bottom of the gel. The membrane transfer was set up by equilibrating 2 sponges and 2 fiber pads for each gel in the western transfer buffer. The membrane (Millipore-Immobilon™ Transfer Membrane, PVDF, 0.45 µM) was activated in methanol before also being equilibrated with western transfer buffer (3.03 g Trizma Base, 14.41 g glycine, 800 mL H_2O, 200 mL methanol). The gels were removed from the gel cases carefully and allowed to equilibrate in the western transfer buffer for about 5

min. A stir bar and ice pack were added to the gel box. The gel sandwich was made in the following order: black side of sandwich, pad, whatman paper, gel, membrane, whatman paper, pad, white side of sandwich. The transfer occurred overnight at 20V, with stirring, and ended with a 15 min 150 V boost in the morning. The membranes were removed carefully and visualized using 100% Ponceau solution to ensure the presence of protein. Once that was established, the membrane was blocked in blocking buffer (TBST, 5% Chicken Albumin) for an hour, and then treated with 3 TBST (20 mM Tris-Cl, 500 mM NaCl, 0.05% Tween 20, 0.2% Triton X-100) washes and 1 TBS (20 mM Tris-Cl, 500 mM NaCl) wash of 5 min each. The membrane was then incubated for an hour with blocking buffer plus rabbit polyclonal anti-prp43 IgG (Santa Cruz Biotechnology, Inc., 200 µg/mL) and goat polyclonal anti-cdc28 IgG (Santa Cruz Biotechnology, Inc., 200 µg/mL) protein with a 1:1000 ratio (i.e. 7 µl of antibody per 7 mL of blocking buffer used. The washes were repeated and the membrane was incubated for an hour at room temp with donkey anti-goat IgG-HRP (Santa Cruz Biotechnology, Inc., 200 µg/0.5 mL) and goat anti-rabbit IgG HRP (Santa Cruz Biotechnology, Inc., 200 µg/0.5 mL) secondary antibodies, with a 1:5000 ratio. After the final washes the membranes were visualized using chemiluminescent detection (Supersignal® West Dura Horseradish Peroxidase) with Kodak film, developer, and fixer.

IV. Results

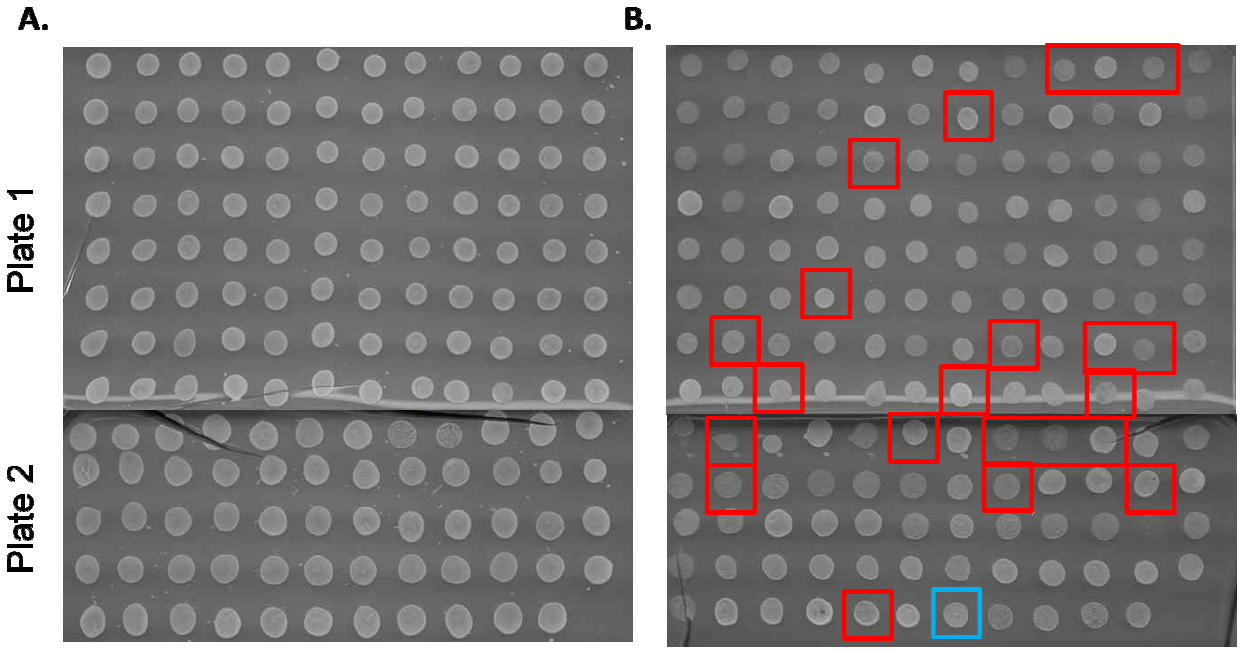

Figure 4. Initial kinase deletion and DNA repair mutant strain screening. Cells were grown by inoculating plates with 7 µl from the working copy. The SD agar plates containing either 100 ul of 100% DMSO (A) or 0.8 mM BPA (B). The plates were incubated at 30°C for 48 hours. The red boxes indicate the strains that were the most consistently sensitive and were chosen for further assays. The blue box indicates the location of the wild type.

Screening of kinase deletion mutants revealed 17 sensitive strains: During the summer of 2010, I worked on this project and generated the preliminary data that was used for my thesis during the spring semester. A working copy of the mat-α haploid deletion library (Open Biosystems) was created selecting only for kinase and DNA repair mutants, resulting in ~180 different deletion strains (See Appendix I). These strains were grown on SD agar in the presence of DMSO only or 1mM BPA and allowed to grow at 30°C for 2 days. This assay was repeated 5 times using both YPD and SD agar and the mutants boxed in (Fig 4) indicate the most consistently sensitive mutants that were chosen for further analysis via spot dilution assays.

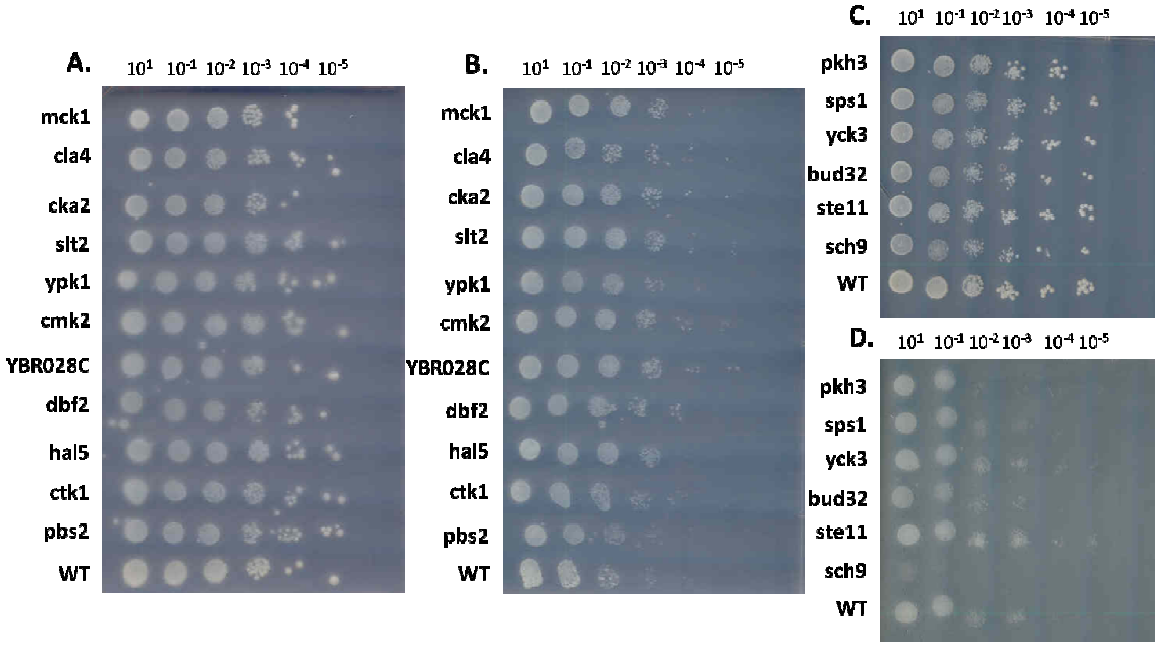

Figure 5. Spot dilution assays of 17 hypersensitive kinase deletion strains. Cells were taken from an overnight inoculate grown in SD media. The cells were diluted to $6x10^6$ cells/mL and then serially diluted by factors of 10 to generate the rest of the spots to a final concentration of 10^1 cells/mL. 7 µl of cells were spotted onto plates containing SD agar and 1 mM BPA (B, D) or 100% DMSO (A, C) of equal volume and allowed to grow for 4 days at 30°C.

Further screening of sensitive strains shows extent of sensitivity: Overnight inoculates were taken and diluted to the same cell concentration and spotted on SD agar plates containing just DMSO or 1 mM BPA (Fig 5). These cell cultures were serially diluted starting with 10-fold dilutions at each step, starting with $6x10^6$ cells/mL. The serial dilutions allow us to have a greater observe the extent of sensitivity to BPA. It appeared that the most sensitive strains were Δpkh3, Δsch9, Δcla4, and Δpbs2 relative to their growth on the DMSO plates, while the putative kinase ΔYBR028C, and Δste11 appear to have growth that is better than the wild type.

Six deletion strains were chosen for in-depth analysis based on their interactions with each other and the high osmolarity glycerol (HOG) pathway in *S. cerevisiae* (Table 1).

Table 1. Gene Summaries. Gene summaries of the 17 genes used for spot dilution assays and further growth analysis. Gene deletion is listed as the gene name, and includes a basic summary of gene function, how many references it contains in literature, as well as interaction with other genes within the table, and total interactions with genes in *S. cerevisiae.* All information was obtained from the Yeast Genome Database (www.yeastgenome.org).

Gene	Function	Literature	Interactions
Mck1	GSK3, chromosome segregation, differentiation, gene expression, meiosis,	74	Cka2, Hal5, Pbs2, (421 total)
Cla4	Cdc42p activated, vacuole inheritance, cytokinesis, phosphorylates Cdc3p and Cdc10 p	134	Slt2, Dbf2, Hal5, Yck3, Ste11, (622 total)
Cka2	roles in cell growth and proliferation	107	Mck1, (325 total)
Slt2	cell wall integrity, progression through the cell cycle,regulated by Pkc1	329	Cla4, Cmk2, (627 total)
Ypk1	downregulates flippase activator Fpk1p, homolog of mammal Sgk	54	Dbf2, (65 total)
Cmk2	may play role in stress response	35	Slt2, Pbs2, Ste11, (47 total)
Dbf2	involved in transcription and stress response, exit from mitosis, activated by Cdc15	109	Cla4, Ypk1, Hal5, (380 total)
Hal5	role in regulation of Trk1p and Trk2p transporters	34	Mck1, Cla4, Dbf2, Pbs2, (164 total)
Ctk1	affects transcription and pre-mRNA 3'end processing	111	Pbs2, Sch9 (276 total)
Pbs2	osmosensing signal transduction pathway, activated under severe osmotic stress	192	Mck1, Cmk2, Hal5, Ctk1, Ste11, (303 total)
Pkh3	suppressor of Pkh1 and Pkh2	10	Sch9 (40 total)
Sps1	expressed at the end of meiosis, localization of enzymes involved in spore wall synthesis	32	37 total
Yck3	regulates vacuole fusion during hypertonic stress	33	Cla4, (46 total)
Ste11	involved in pheremone response and pseudohyphal/invasive growth pathways	299	Cla4, Cmk2, Pbs2, (183 total)
Vps34/15	regulates protein sorting	162	
Bud32	bud site selection, telomere uncapping elongation, and transcription	32	
Sch9	transcriptional activation of osmostress responsive genes, G1 progression,	155	Ctk1, Pkh3

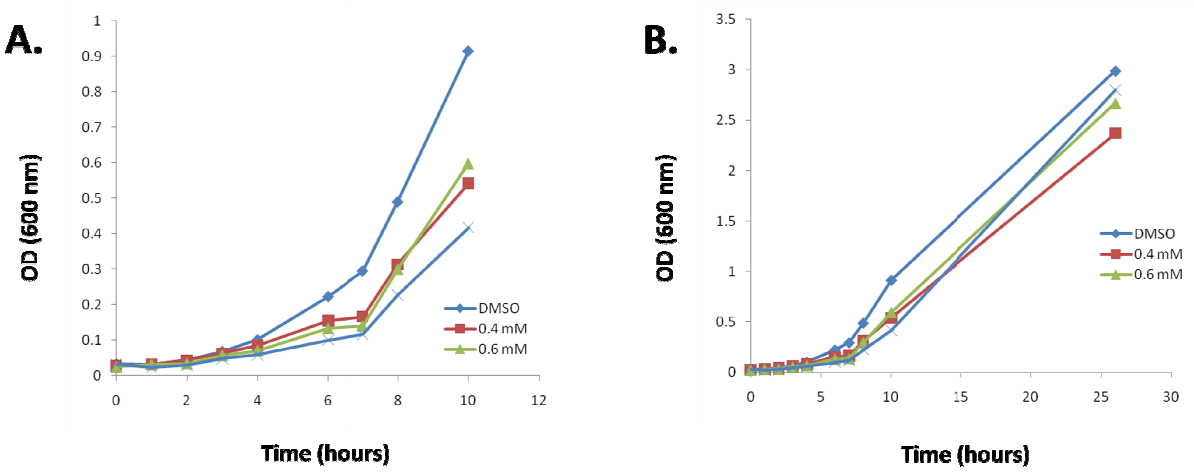

Figure 6. Growth response and adaptation of wild type yeast to different concentrations of BPA. An overnight inoculate of the wild type strain was diluted to a final cell number of $4.5x10^5$ cells per mL in 10 mL of SD media. Cells were incubated at 30°C and allowed to grow to a cell number of approximately $1x10^6$ cells per mL and 0.8 mM, 0.6 mM, 0.4 mM BPA or DMSO was added to the media. Time points were then taken over the course of 10 hours (A) and 24 hours (B).

Liquid growth curve response of wild type in liquid assay reveals inhibitory concentration and the possibility of adaptation: When I first tried to conduct liquid growth curve assays, I realized that the concentration of BPA was so high that the mutant strain was not able to recover from the stress. I conducted an assay to calculate the inhibitory concentration of BPA where 50% of cells survive as compared to the control. I used DMSO, 0.4, 0.6, and 0.8 mM of BPA in SD media and observed the growth over a period of 10 hours. The final concentrations of the cultures were then used to calculate the percent survival, by using the value of the strain with 0 mM BPA as 100% growth. It was calculated that 0.8 mM BPA was close to the IC-50 of wild type *S. cerevisiae* and from then on was the concentration of BPA used in all liquid assays. The 0.4 and 0.6 mM values appear to have over lapped at hour 8 (6, A) and the 0.8 mM and the 0.6 value surpass the value of the strain growing in 0.4 mM (6, B), suggesting that at some point after 10 hours, the strain is able to adapt to the BPA induced stress.

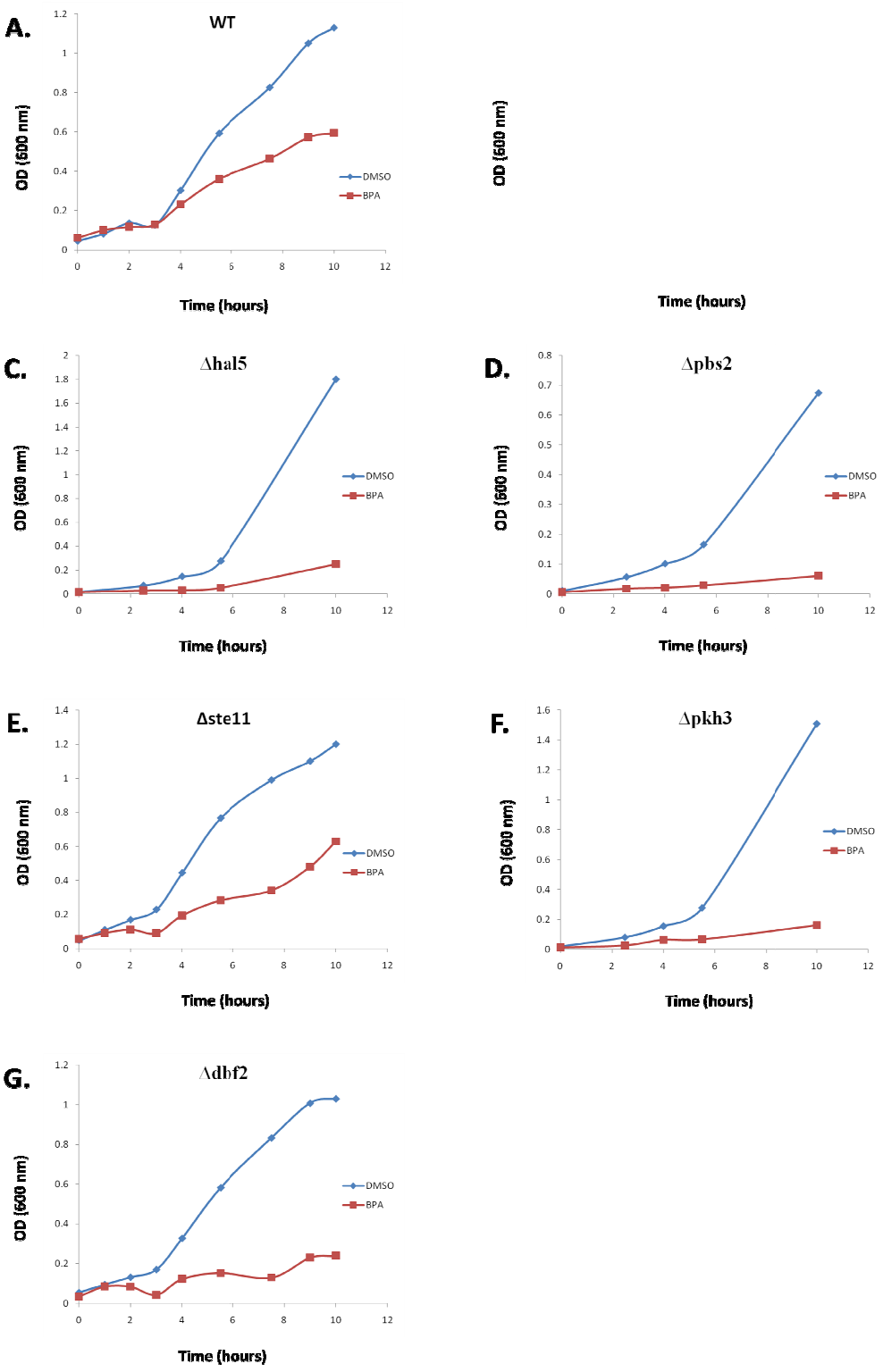

Figure 7. Growth Curves of kinase deletion mutants involved in the high osmolarity glycerol pathway. Overnight inoculates of the kinase deletion strains: WT (A), Δmck1 (B), Δhal5 (C), Δpbs2 (D), Δste11 (E), Δpkh3 (F), and Δdbf2 (G) were diluted to a final cell number of 4.5 cells per mL in 10 mL SD media. Cells were incubated at 30°C and allowed to grow to a cell number of approximately $1x10^6$ cells per mL and 0.8 mM BPA or DMSO was added to the media. Time points were then taken over the course of 10 hours.

While the concentration of BPA I used is slightly higher than has been used in other studies in non yeast systems, we are still within the range of what Iso et al 2006. used for their studies on mammalian cells. They used a range of 10^{-6}-10^{-4} M BPA, and the value used in this lab was approximately $8x10^{-4}$. There could be a number of reasons for this shift in concentration needed to produce an inhibitory concentration of IC-50, but I believe that it is because yeast has a cell wall and lacks estrogen receptors on its surface which would enable BPA to exert additional hormonal effects on the cell. It has also been shown that the effects of BPA in mammalian cells are very tissue specific, so it is not surprising that a non mammalian cell would have different tolerances to BPA (Wetherill, 2007).

Growth curves of mutants related to high osmolarity glycerol pathway shows variation in sensitivity with regards to time: The high osmolarity glycerol pathway has been implicated as a potential defense mechanism in response to the presence of BPA. It is generally associated with osmotic stress response and stimulates the production of glycerol to balance changes in the osmotic gradient. The growth of 6 kinase deletion mutants which are involved in this osmotic stress response was observed over 10 hours (Fig 7). The Δmck1, Δste11, and Δdbf2 deletion strains had growth phenotypes close, and slightly closer, respectively, to that of wild type, suggesting that these mutants may have some way of adapting to the stress caused by BPA. However, this could also be due to the fact that with a greater concentration of cells, more BPA is being metabolized and broken down. In contrast, the other three strains only had a survival rate of 14% or less, showing that they obviously could not recover (Table 2).

Table 2. Final OD_{600} values of kinase mutants and percent survival. The final OD_{600} values of kinase deletion mutants growing in the presence of DMSO or 0.8 mM BPA at 10 hours of growth was taken. The OD_{600} value of growth in BPA was used to generate percent survival, with the OD_{600} value of growth in DMSO equaling 100% growth.

Strain	DMSO	BPA	% Survival
WT	1.13	0.595	53
Mck1	0.318	0.112	35
Hal5	1.8	0.25	14
Pbs2	0.675	0.061	9
Ste11	1.2	0.63	52
Pkh3	1.51	0.161	11
Dbf2	1.03	0.24	23

Liquid Growth assay of 17 hypersensitive strains in differing concentrations of BPA provides further support to findings of solid growth assay: The difference between these assays and the liquid growth curve is that the growth of the strains was not observed continuously over 10 hours, and they were not given the chance to revitalize (the growth of 2.5-3 hours before adding the compound). The growth of kinase deletion mutants were observed after 17 hours in the presence of 0.6, 0.8, and 1 mM BPA (Fig 8). While most strains ended up with similar percent survival as the wild type in the presence of 0.8 mM BPA after 17 hours, they all had differing and conflicting reactions to lower doses of BPA. The OD_{600} values of each strain versus concentration of BPA can be found in Appendix II. It is at these lesser concentrations of BPA that differences in sensitivity can truly be seen. The strain that stands out the most is the Δhal5 strain. It was observed that the Δhal5 strain, under control conditions, has a higher growth rate than the wild type (see DMSO treatment values in Fig 7of Δhal5 and wild type). This could mean that Δhal5 is also able to recover from the presence of BPA, although it might take longer than Δste11, Δmck1, and Δdbf2. It can then

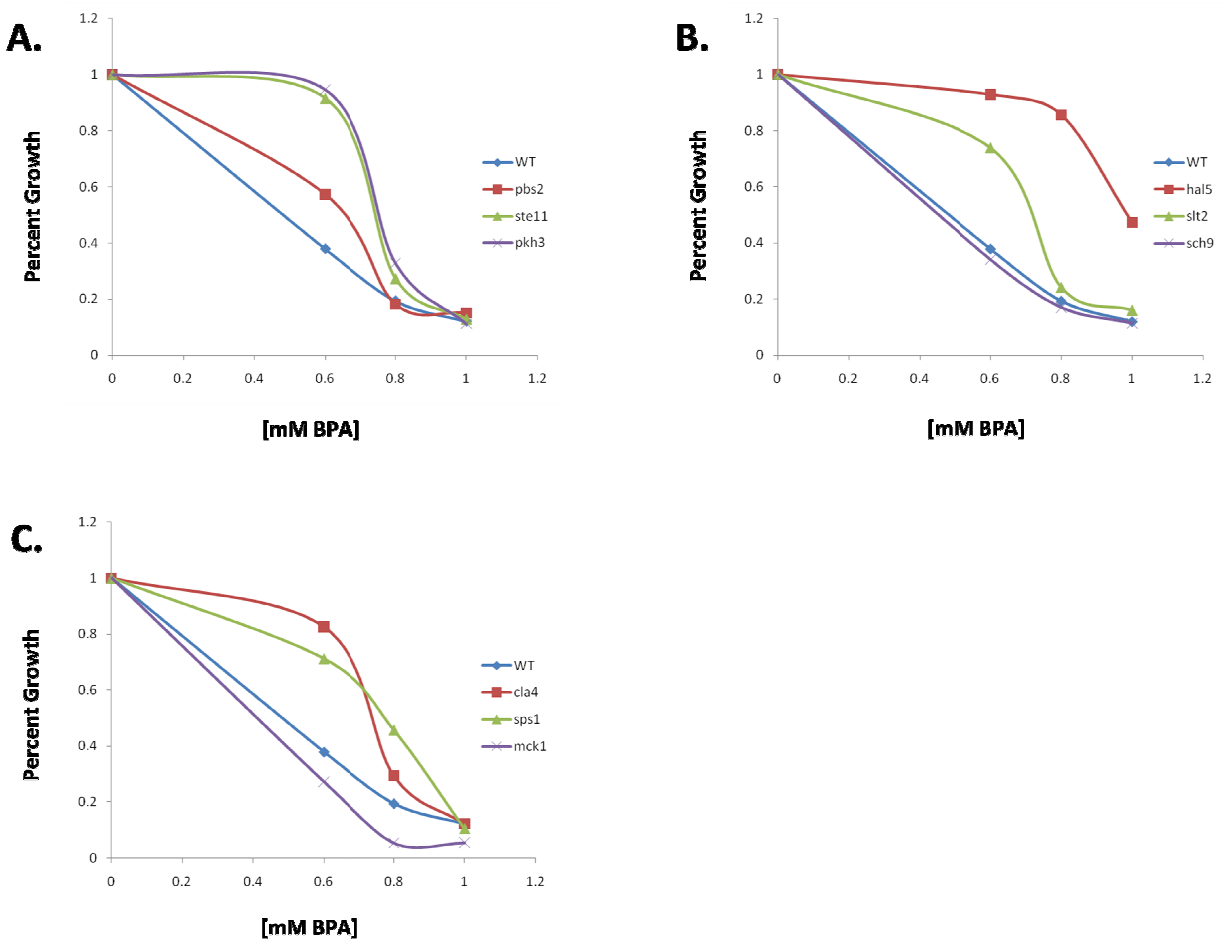

Figure 8. Growth Assays of mutants in different concentrations of BPA after 17 hours. Overnight inoculates of kinase deletion mutants used for the spot assays were diluted to a final cell number of $1.5x10^6$ cells per mL in 200 µl SD media. 1 mM, 0.8 mM, 0.6 mM and DMSO was added to the cells and they were distributed to 96 well plates, in duplicate. Cells were incubated at 30°C and allowed to grow for 17 hours overnight, with spinning. Readings were taken via plate reader, and the OD_{600} values are the average of 3 readings and duplicates. Growth in DMSO was set to 100% growth and the percent growth of the other concentrations of BPA was calculated. Wild type is displayed for comparison on all three graphs.

regain its extremely fast growth rate to end up with a higher percent of growth than the wild type strain. The other possibility is that after 17 hours, the DMSO only treated Δhal5 strain could have reached saturation, and thus growth was halted, allowing for the strains treated with BPA to catch up.

It is interesting to note how in the Δste11, Δpkh3, and Δcla4 deletion strains, the 0.6 mM BPA treated cells do not appear as severely affected as those cells treated with higher concentrations of BPA, and the severity is shown in the slope of the graphs. Perhaps the 0.6

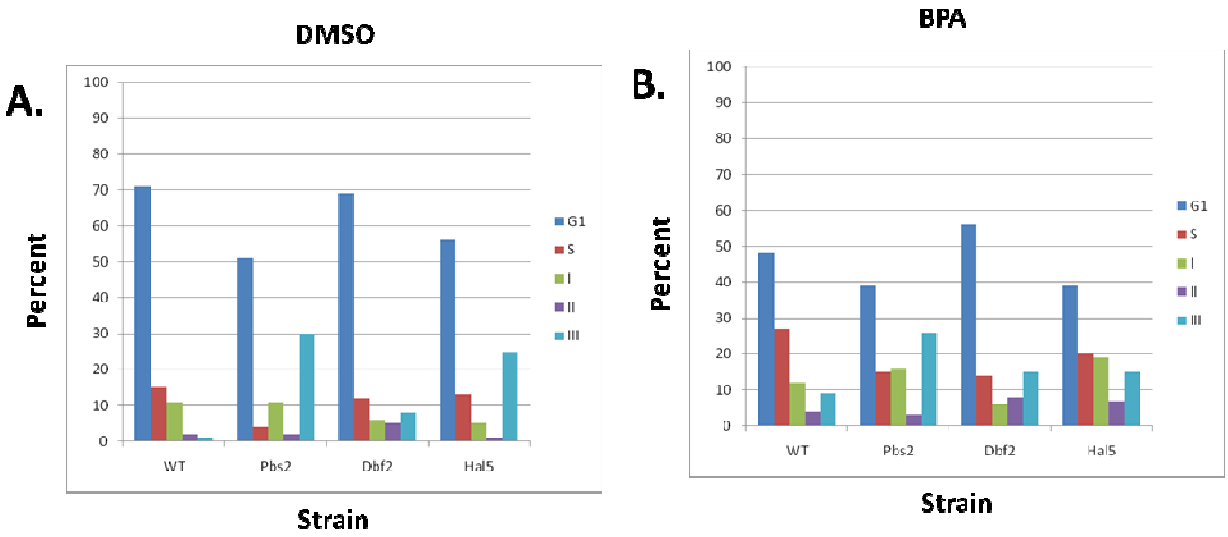

Figure 9. Cell cycle stages of kinase deletion mutants. Overnight inoculates were diluted to a cell number of $1.5x10^6$ cells per mL and grown overnight with DMSO and 0.8 mM BPA. DMSO treated cells (A) and BPA treated (B) cells were stained with DAPI and visualized under a fluorescence microscope to determine cell cycle stages using a combination of bright field images and nucleic fluorescence. At least 100 cells were observed for every strain and condition.

mM BPA treatment is just low enough not to kill too many cells, while allowing the strain to adapt to the new stressor and thus eventually resume its normal growth. It would be very interesting to repeat the growth curve assays using 0.6 mM BPA instead of 0.8 mM BPA. The Δmck1 strain appears to have a greater sensitivity than the wild type strain, which contradicts the data from the growth curves in figure 7. A possible explanation for this is that perhaps the Δmck1 strain is only able to recover so much, and that this small recovery becomes more apparent after 17 rather than 10 hours. The recovery of the strain could plateau while the DMSO only treated strain continues to grow in a logarithmic form, resulting in the disparity between the percent survival between those two strains.

Fluorescence microscopy shows cell cycle interruption in the presence of BPA: The cells were analyzed microscopically with DAPI staining and the cell cycle distribution of the strains was observed (Fig 9). The cells were classified based on what stage of the cell cycle

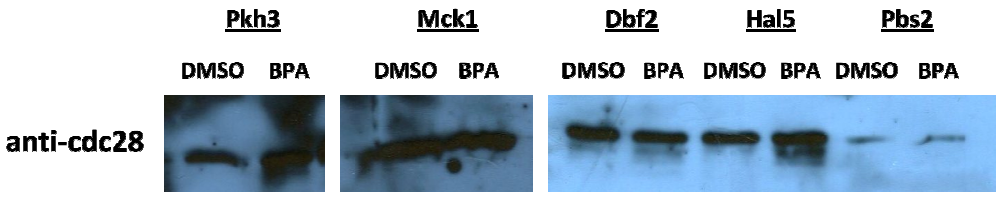

Figure 10. Western Blot analysis of Cdc28 expression. Cells were grown overnight in the presence of DMSO or 0.8 mM BPA. Approximately $9x10^7$ cells were harvested and protein was extracted. The protein extract was then analyzed using SDS-page and Cdc28 antibody to determine Cdc28 expression.

they were in, G1, S, or G2, which was further divided into three classes: (class I) an undivided nucleus in one cell body. (class II) undivided nucleus in the bud neck. (class III) divided nuclei in two cell bodies (see figure 3) (Niu, 2008). Generally, DNA replication occurs when the bud size is small, nuclear division occurs when the bud is about ¾ the size of the mother cell, and cell division occurs when they are equal in size (Niu, 2008). By combining the nuclear morphology observation with bud morphology, one can determine what stage of the cycle cells are in with greater accuracy. All four of these strains displayed shifts in their cell cycle stages. The greater distribution of cells was always in G1 in control conditions, but there is a shift in the number that are in the S and G2/I and G2/II stages. This might suggest that the cells are having difficulty completing mitosis and thus are stuck in the early stages of G2.

Total Cdc28 content is unaffected by BPA: The following strains were treated with BPA or DMSO overnight and protein was extracted to determine Cdc28 expression: Δpkh3, Δmck1, Δdbf2, Δhal5, Δpbs2. There were air bubbles on the gel that included the WT strain, among others, which is why the wild type strain is not included. This assay needs to be repeated. It appears that the presence of BPA is not making a large impact on the total content of Cdc28, indicating that it must be affecting the cell cycle in other ways than regulation of expression. The BPA treated lanes in the Δpkh3, Δdbf2, and Δhal5 strains show

the presence of smaller Cdc28 protein, which might suggest that BPA could be impacting the phosphorylation states of Cdc28.

V. Discussion

I applied a systematic approach to identify a candidate pathway involved in the adaptation of *S. cerevisiae* to BPA. Using solid growth assays, I was able to identify seventeen sensitive haploid mutants, six of which were related to the high osmolarity growth (HOG) pathway and osmotic stress response. These strains were studied further with liquid growth assays, protein analysis, and cell cycle assessment.

The HOG pathway is one of the mitogen activated protein kinase pathways (MAPK) in yeast. MAPK pathway cascades are essential for *S. cerevisiae* to respond to extracellular and intracellular signals, by regulating transcription factors via phosphorylation (Gustin, 1998). There are five distinct MAPK pathways that can be found in *S. cerevisiae*: pheromone response, filamentation/invasion, high osmolarity growth pathway, cell integrity, and spore wall assembly (Gustin, 1998). They all generally act through the same mechanism, MAPK cascades have been found to exist in the cytoplasm in macromolecular complexes with other proteins serving as scaffolds, anchors, or adaptors, and move into the nucleus upon activation in order to phosphorylate transcription factors (Gustin, 1998).

Most cells adapt to increases in osmolarity by producing small solutes that help balance the osmotic gradient between the cell and its environment (O'Rourke, 2002). This response in *S. cerevisiae* is mediated by the HOG pathway. In general, the internal osmolarity of cells is kept higher than the external osmolarity, which generates a gradient that ensures that water continually enters the cell and creates turgor (Gustin, 1998). It is thought that the HOG pathway is activated by osmosensors through changes in the turgor pressure of the cell, and reacts by targeting several genes, including GDP1, which is glycerol-3-phosphate dehydrogenase and catalyzes the glycerol synthesis from

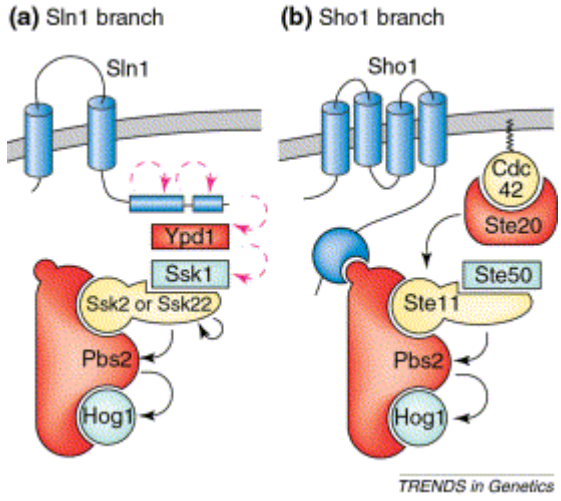

Figure 11. The two branches of the HOG pathway (O'Rourke).

dihydroxyacetone phosphate (Gustin, 1998). It has been shown that the HOG pathway is activated by increasing the concentration of several solutes, so that it is truly sensitive to only osmolarity changes instead of glycerol levels, specifically (Gustin, 1998).

The main MAPK kinases in the HOG pathway are Pbs2 and Hog1. Pbs2 acts as a scaffold to activate Hog1 and thus allows it to be transported into the nucleus where it can activate the transcription of several genes(O'Rourke, 2002). It has been shown that mutations in Pbs2 cause osmosensitivity and accumulation of reduced levels of glycerol, showing that it is a key factor in the stimulation of the production of glycerol and thus a key player in reaction to stress (O'Rourke, 2002). The Hog1 kinase cannot be activated without Pbs2, which doesn't allow it to be transported into the nucleus, which would be seriously detrimental to the cell. This explains why the Δpbs2 mutant strain was never able to really recover from the presence of BPA. It displayed great sensitivity in all assays, with 9% survival in the liquid growth curve (Fig 7, Table 2), similar sensitivity as the wild type to different concentrations of BPA (Fig. 8), and apoptotic cells observed in fluorescence. DNA

microarray studies have shown that Hog1 can significantly regulate the expression of ~600 genes (O'Rourke, 2002). Thus the absence of the Pbs2 gene would have immense effects on the cell's ability to use this pathway to counteract exposure to BPA.

In general, the HOG pathway can be activated by two different branches, the Sln1 branch and the Sho1 branch (Figure 11). The two branches are used interchangeably in responses to different levels of stress. When exposed to moderate amounts of stress the Sln1 branch is used specifically to activate the pathway, while the Sho1 branch is only used during extreme osmotic stress and is thus dispensable under most growth conditions (Westfall, 2004). Pbs2 interacts directly with Ste11, working as a scaffold protein link to Sho1, which could limit the cross talk between the pheromone response pathway, for which Ste11 is also used. This might be able to explain why the Δste11 strain is able to eventually adapt to the presence of BPA, because this pathway is a two part pathway, and Ste11 is used for other processes other than osmotic stress response. Although the Ste11 kinase gene is deleted, the cell is still able to utilize the Sln1 branch.

The Sln1 branch is a histidine kinase branch and is comprised of a phosphorelay system where a histidine kinase protein transfers a phosphate group to an intermediate, which will then transfer the phosphate to another protein (O'Rourke, 2002). This would show that the cascade does not work via amplification and would have to be highly regulated. The Sln1 branch works though negative regulation when the basal osmotic levels are normal; activation occurs through the dephosphorylation of these proteins. Sln1 actively phosphorylates Ypd1, which transfers the group to Ssk1, which cannot form the complex required to interact with Pbs2 (O'Rourke, 2002). When the branch gets activated, the kinase

activity of Sln1 becomes inhibited, which allows the formation of the Ssk1-Ssk2/22 complex (O'Rourke, 2002).

Further down the pathway, Hog1 enters the nucleus and can activate the transcription of 3 genes which are involved in the production of glycerol. The main pathway that is used results in the activation of the GPD1 promoter, but the activation of CTT1 is very important as well. CTT1 is regulated by the interaction of Hog1 and Msn2 or Msn4, which are important for nuclear retention of Hog1 in the nucleus as well (O'Rourke, 2002). One of the kinase deletion mutants, Δmck1, has been implicated in the binding of the Msn2 zinc finger transcriptional domain to the stress response genes (Hirata, 2003). The Δmck1 kinase deletion mutant has also shown some adaptation to the presence of BPA; the fact that the Hog1 protein can use either Msn2 or Msn4 to activate this gene means the branch of the pathway wouldn't be completely obstructed through the deletion of Mck1. Hog1 can also activate the transcription of many other genes, so the deletion of Mck1 is not far enough up the pathway to cause a great effect.

Apart from controlling the stress induced expression of genes, the HOG pathway has also been shown to have roles in cell morphogenesis and the cell cycle (Gustin, 1998). Cell cycle progression in *S. cerevisiae* is affected by osmotic stress. Alexander et al. 2001 studied the effects of the cell cycle delays due to the HOG pathway and its effects on the activities of the Cdc28 kinase. They found that osmotic shock causes an accumulation of cells in the G1 and G2 phases of the cell cycle. The increase in external osmolarity causes an accumulation of 1N and 2N cells and a depletion of S cells (Alexander, 2001). While observations of cell cycle distribution revealed more cells in S phase as well as G2 (Fig. 9), these results could be

resolved by conducting a more quantitative form of cell cycle analysis, such as flow cytometry.

The progression of the cell cycle is driven by the Cdc28 kinase; it associates with activating subunits known as cyclins in order to trigger the next stages in the cell cycle. Cdc28 associates with α-cyclins in G1 and β-cyclins in G2. Alexander et al. 2001 have also shown that the levels of Cdc28 are not altered, while the phosphorylation state of the protein is affected by stress, which is consistent with the western blot results in Figure 10 (Alexander, 2001). Alexander states that "the Hog1 dependent inhibition of Clb2p-Cdc28p kinase activity is puzzling in light of the finding that cell cycle progression is significantly slowed, if not completely delayed, even though Clb2p-Cdc28p activity remains high following hypertonic stress" (Alexander, 2001). The actual mechanism by which Hog1 regulates the activity of Cdc28 is not known at this time, and would be a good candidate for further investigation.

The HOG pathway is also very closely related to the calcineurin pathway, which regulates ion homeostasis. This is reflected the results by the identification of the Δhal5 mutant strain as sensitive to BPA. Hal5 helps regulate ion homeostasis in response to salt stress (www.yeastgenome.org). The calcineurin pathway is essential as a signal pathway for HOG by regulating ionic homeostasis, whose ultimate target is the ENA1 gene, a p-type ATPase (Matsumoto, 2002). The increased expression of ENA1 occurs in conjunction with salt stress; generally transcription levels are kept low until exposed to stress (Proft, 1999). This gene is also negatively regulated by Hog1, suggesting that there must be some type of cross talk between the calcineurin pathway and the HOG pathway to provide a combined

ionic and osmotic response to stressors(Proft, 1999). Indeed, in Table 1. we can see that Hal5 interacts with Pbs2, the primary activator of Hog1.

In *S. cerevisiae*, osmotic shock causes the influx of Ca^{2+} which enhances the adaptation of yeast to ionic but not osmotic stress (Matsumoto, 2002). It has been shown that Δhog1 deletion mutants repress the reporter genes more strongly, and are unable to remove the negative regulators from the promoter gene (Proft, 1999). This is reflected in the results by the hypersensitivity of the Δpbs2 mutant. Contrastingly, in an Δmsn2Δmsn4 double mutant, direct negative regulators of ENA1, the expression of ENA1 was unaffected when confronted to stresses as compared to the wild type (Proft, 1999). This observation is reflected in the results by the apparent resistance of Δmck1 to BPA, as compared to wild type.

BPA has been implicated in interactions with cellular enzyme targets in both fish and mammals, specifically Ca^{2+} ATPases, which keep the intracellular concentrations of calcium low (Kirk, 2003). It has been shown that alkylphenols affect calcium homeostasis by inhibiting the intracellular calcium pump, disallowing the release of calcium to the extracellular environment (Hughes, 2000). This rapid increase in Ca^{2+} ions could be one of many triggers of stress response to BPA. This also means that BPA may also inhibit the activity of related pumps and pumps that regulate the gradients of other ions.

VI. Conclusion:

In this study, I followed the pathway/target identification procedure that was outlined by Baetz et al. 2004. I conducted a systematic screen of yeast kinase deletion mutants using the drug induced phenotype of growth inhibition. Through this screen I identified a potential pathway used in resistance to the presence of BPA. I tested the growth phenotypes of these deletion mutants on solid assays as well as liquid assays. I measured the extent of sensitivity using spot dilution assays as well as differing amounts of BPA in liquid growth assays. I visualized cell cycle delays using fluorescence microscopy and the DAPI stain as well as observe the expression of the Cdc28 protein.

The next steps in the process would be to verify my findings using high throughput analyses. There is bound to be some error and bias in my observations, since the spot assays and cell cycle arrests were analyzed by visual inspection. For example, I did not identify the Δhog1 kinase mutant as hypersensitive (Figure 4, Plate 1, spot A-5), although it would be expected that it would display the same phenotypes as the Pbs2 mutant, since they are both integral to the Hog pathway activation. As Niu observed, the mutations caused by loss of function, or deletion, can be masked such as through negative regulators, which is what is believed to be the mode of regulation for the HOG pathway. Therefore I propose that studies observing overexpression phenotypes should also be used to confirm my data, as well as provide additional insight to the sensitivity of these mutants to BPA. Since the HOG pathway relies on increases in glycerol levels in order to restore osmotic balance, the sensitivity of these strains should also be verified using assays measuring changes in glycerol levels. It would also be very interesting to see if sensitivity of these mutants is also correlated with

changes in the phosphorylation of targets of these kinases. Since some of these kinases have been observed to naturally inhabit the cytosol, and being transported into the nucleus during stress, an assay studying the localization of these proteins (or their targets) such as FISH would also be very helpful. Ultimately, the homologs of genes in this pathway should be studied in mammalian cells.

Acknowledgements

Ultimately, I would like to thank Dr. Edwalds-Gilbert for mentoring me for the past 4 years, for her support, and belief in my abilities. Working in her lab encouraged me to pursue a career in science, and I am eternally grateful. I also thank my lab mates: Betsy Martin as my comrade in BPA research, as well as Vivian Maltez, Laura Hoverson, Lizzie Meier, and Catherine Gilbert for their moral support and comic relief. This research would not have been possible without the collaboration of Dr. Tina Negritto, of Pomona College and Tyler Petersen, Pomona ‘11.

References:

Alexander MR, Tyers M, Perret M, Craig BM, Fang K, Gustin MC. (2001) Regulation of Cell Cycle Progression by Swe1p and Hog1p Following Hypertonic Stress. Molecular Biology of the Cell. 12: 53-62.

Baetz K, McHardy L, Gable K, Tarling T, Rebérioux D, Bryan J, Anderson RJ, Dunn T, Hieter P, Roberge (2004) Yeast genome-wide drug-induced haploinsufficiency screen to determine drug mode of action. PNAS 101: 4525-4530.

Breitkrutz *et al. .(2010)* A Global Protein Kinase and Phosphotase Interaction network in Yeast. Science 328:1043-1046.

Calafat AM, Ye X, Wong L, Reidy JA, Needham LL (2008) Exposure of the U.S. Population to Bisphenol A and 4-*tertiary*-Octylphenol: 2003-2004. Environmental Health Perspectives 116: 39-44.

Calvert MEK, Lannigan JA, Pemberton LF. (2008) Optimization of Yeast Cell Cycle Analysis and Morphological Characterization by Multispectral Imaging Flow Cytometry. Cytometry Part A. 73A: 825-833.

Gustin MC, Albertyn J, Alexander M, Davenport K. (1998) MAP Kinase Pathways in the Yeast *Saccharomyces cerevisiae.* Microbiology and Molecular Biology Reviews. 62: 1264-1300.

Hirata Y, Andoh T, Asahara T, Kikuchi A. (2003) Yeast Glycogen Synthase Kinase-3 Activates Msn2p-dependent Transcription of Stress Responsive Genes.

Hughes PJ, McLellan H, Lowes DA, Khan SZ, et al. (2000). Estrogenic Alkylphenols Induce Cell Death by Inhibiting Testis Endoplasmic Reticulum Ca^{2+} pumps.

Iso T, Watanabe T, Iwamoto T, Shimamoto A, Furuichi Y. (2006) DNA Damage Caused by Bisphenol A and Estradiol through Estrogenic Activity. Biol. Pharm. Bull. 29: 206-210.

Kirk CJ, Bottomley L, Minican N, Carpenter H, Shaw S, et al. (2003). Environmental endocrine disrupters dysregulate estrogen metabolism and Ca^{2+} homeostasis in fish and mammals via receptor-independent mechanisms. Comparative Biochem. and Physio. Part A. 135: 1-8.

Krishnan AV, Stathis P, Permuth SF, Tokes L, Feldman D. (1993) Bisphenol-A: An Estrogenic Substance is Released from Polycarbonate Flasks during Autoclaving. Endocrinology. 132: 2279-2285.

Levy ED, Landry CR, Michnick SW (2010) Signaling Through Cooperation. Science 328: 983-984.

Matsumoto TK, Ellsmore AJ, Cessna SG, et al. (2002). An Osmotically Induced Cytosolic Ca^{2+} Transient Activates Calcineurin Signaling to Mediate Ion Homeostasis and Salt Tolerance of *Saccharomyces cerevisiae.* Journal of Bio. Chem. 277:33075-33080.

Niu W, Li Z, Zhan W, R. lyer V, Marcotte E (2008) Mechanisms of Cell Cycle Control Revealed by a Systematic and Quantitative Overexpression Screen in *S. cerevisiae.* PLoS Genetics 4; 7: 1-15.

O'Rourke SM, Herskowitz I, O'Shea E. (2002) Yeast go the whole HOG for the hyperosmotic response. TRENDS in Genetics. 18: 405-412.

Proft M, Serrano R. (1999) Repressors and Upstream Sequences of the Stress Regulated *ENA1*Gene in *Saccharomyces cerevisiae:* bZIP Protein Sko1p Confers HOG-Dependent Osmotic Regulation. Mol. and Cell Bio. 19:537-546.

Völkel W, Colnot T, Csanády GA, Filser JG, Dekant W. (2002) Metabolism and Kinetics of Bisphenol A in Humans at Low Doses Following Oral Administration. Chem. Res. Toxicol. 15: 1281-1287.

Walsh DE, Dockery P, Doolan CM. (2005). Estrogen receptor independent rapid non-genomic effects of environmental estrogens on [Ca^{2+}] in human breast cancer cells. Mol. and Cell Endocrinology 230:23-30.

Westfall PJ, Ballon DR, Thorner J. (2004) When the Stress of Your Environment Makes You go HOG Wild. Science 306: 1511-1512.

Wetherill YB, Akingbemi BT, Kanno J, McLachlan JA, et al (2007). *In vitro* molecular mechanisms of bisphenol A action. Reproductive toxicology 24:178-198.

Figure 1: http://rheothing.blogspot.com/2010/09/bpa.html

Appendix I. Kinase Deletion Plate Gene Locations

Plate	Row	Well	gene name	systematic name	Plate	Row	Well
1	A	1	psk1	YAL017W	101	D	2
1	A	2	kin3	YAR018C	101	E	6
1	A	3	kns1	YLL019C	101	G	7
1	A	4	kin2	YLR096W	102	F	11
1	*A*	*5*	hog1	YLR113W	102	s	10
1	A	*6*	sky1	YMR216C	104	E	1
1	A	7	tda1	YMR291W	105	A	2
1	A	8	mck1	YNL307C	105	D	4
1	A	9	cla4	YNL298W	105	D	11
1	*A*	10	cka2	YOR061W	106	D	2
1	A	11	mek1	YOR351C	107	B	4
1	A	12	psk2	YOL045W	107	G	2
1	B	1	env7	YPL236C	108	D	7
1	B	2	tpk2	YPL203W	108	F	4
1	B	3		YPL150W	109	B	1
1	B	4		YPL141C	109	B	6
1	B	*5*	mkk2	YPL140C	109	B	7
1	B	*6*	kin1	YDR122W	110	G	12
1	B	7	slt2	YHR030C	114	A	8
1	B	8	ire1	YHR079C	114	C	10
1	B	9	ksp1	YHR082C	114	D	1
1	B	10	yck1	YHR135C	114	F	11
1	B	11	kcc4	YCL024W	115	C	3
1	B	12	sat4	YCR008W	115	F	2
1	C	1	pan3	YKL025C	116	E	11
1	C	2	elm1	YKL048C	116	G	3
1	C	3	hsl1	YKL101W	117	B	8
1	C	4	prr1	YKL116C	117	C	5
1	C	*5*	ypk1	YKL126W	117	D	1
1	C	*6*		YKL161C	117	F	2
1	C	7	tpk3	YKL166C	117	F	6
1	C	8	kkq8	YKL168C	117	F	8
1	C	9		YKL171W	117	F	9
1	C	10	fmp48	YGR052W	117	H	12
1	C	11	mkk1	YOR231W	119	D	2
1	C	12	kin4	YOR233W	119	D	3
1	D	1	swe1	YJL187C	119	G	12
1	D	2	tpk1	YJL164C	120	A	3

1	D	3	ste20	YHL007C	121	E	10
1	D	4	rck2	YLR248W	121	H	5
1	D	*5*	ssn3	YPL042C	123	F	8
1	D	*6*	pho85	YPL031C	123	G	5
1	D	7	sks1	YPL026C	123	G	8
1	D	8	isr1	YPR106W	124	A	9
1	D	9	dbf20	YPR111W	124	A	11
1	D	10	kin82	YCR091W	124	G	6
1	D	11	alk2	YBL009W	125	F	1
1	D	12	fus3	YBL016W	125	F	7
1	E	1	tel1	YBL088C	126	C	5
1	E	2	alk1	YGL021W	126	D	11
1	E	3	pkp2	YGL059W	126	G	1
1	E	4	scy1	YGL083W	126	H	7
1	E	*5*	npr1	YNL183C	127	C	12
1	E	*6*	yck2	YNL154C	127	E	2
1	E	7	ptk1	YKL198C	127	E	6
1	E	8	vhs1	YDR247W	128	B	8
1	E	9	gcn2	YDR283C	128	E	5
1	E	10	cka1	YIL035C	129	B	5
1	E	11	prk1	YIL095W	129	D	8
1	E	12	cmk1	YFR014C	129	H	4
1	F	1	pkh2	YOL100W	131	B	9
1	F	2	skm1	YOL113W	131	C	10
1	F	3	ygk3	YOL128C	131	D	9
1	F	4	cmk2	YOL016C	132	C	5
1	F	*5*	smk1	YPR054W	133	D	2
1	F	*6*	ime2	YJL106W	133	H	1
1	F	7	bck1	YJL095W	133	H	6
1	F	8	iks1	YJL057C	134	B	3
1	F	9	bub1	YGR188C	134	F	4
1	F	10	prr2	YDL214C	136	F	12
1	F	11	ptk2	YJR059W	138	E	6
1	F	12	dun1	YDL101C	138	F	2
1	G	1	pkp1	YIL042C	139	F	7
1	G	2		YBR028C	140	B	9
1	G	3	akl1	YBR059C	140	D	12
1	G	4	ark1	YNL020C	140	G	6
1	G	*5*	ssk2	YNR031C	141	C	8
1	G	*6*	fpk1	YNR047W	141	D	9

1	G	7	kss1	YGR040W	143	B	7
1	G	8	dbf2	YGR092W	143	C	1
1	G	9	yak1	YJL141C	143	D	4
1	G	10	hal5	YJL165C	143	D	10
1	G	11	ctk1	YKL139W	143	E	10
1	G	12	rim11	YMR139W	144	E	9
1	H	1	hrk1	YOR267C	144	H	9
1	H	2	ssk22	YCR073C	144	B	6
1	H	3	pbs2	YJL128C	145	C	9
1	H	4	ypk2	YMR104C	145	D	12
1	H	*5*		YDL025C	146	E	2
1	H	*6*	mrk1	YDL079C	146	H	9
1	H	7	pkh3	YDR466W	147	C	8
1	H	8	pkh1	YDR490C	147	E	1
1	H	9	gin4	YDR507C	147	F	1
1	H	10	sps1	YDR523C	147	G	3
1	H	11	rck1	YGL158W	148	C	1
1	H	12	tos3	YGL179C	148	D	6
2	A	1	atg1	YGL180W	148	D	7
2	A	2	yck3	YER123W	148	F	4
2	A	3	sak1	YER129W	148	F	7
2	A	4	tor1	YJR066W	149	C	4
2	A	*5*	snf1	YDR477W	149	D	6
2	A	*6*	ste11	YLR362W	149	G	7
2	A	7	rim15	YFL033C	150	A	8
2	A	8	vps34	YLR240W	171	A	2
2	A	9	vps15	YBR097W	171	C	10
2	A	10	bud32	YGR262C	171	D	4
2	A	11	ste7	YDL159W	172	C	4
2	A	12	cdc5	YMR001C	173	D	3
2	B	1	chk1	YBR274W	175	A	6
2	B	2	sch9	YHR205W	175	F	9
DNA Repair Mutants			**HR**				
2	B	3	YDR369C	*xrs2*	111	C5	
2	B	4	YMR224C	*mre11*	104	E6	
2	B	5	YBR073W	*rdh54*	140	E11	
2	B	6	YGL163C	*rad54*	148	C6	
2	B	7	YDL059C	*rad59*	146	G4	
2	B	8	YML032C	*rad52*	103	C4	
2	B	9	YDR004W	*rad57*	137	A4	

2	B	10	YDR076W	*rad55*	110	E3	
2	B	11	YER095W	*rad51*	131	F3	
2	B	12	YNL250W	*rad50*	132	B12	
2	C	1	YDR386W	*mus81*	111	D5	
			NER				
2	C	2	YER173W	*rad24*	149	A2	
2	C	3	YEL037C	*rad23*	112	A7	
2	C	4	YDR217C	*rad9*	121	B5	
2	C	5	YMR201C	*rad14*	104	D4	
2	C	6	YML095C	*rad10*	132	D6	
2	C	7	YJR052W	*rad7*	138	D12	
2	C	8	YER162C	*rad4*	148	H7	
2	C	9	YGR258C	*rad2*	150	B3	
2	C	10	YPL022W	*rad1*	123	G12	
2	C	11	YKL113C	*rad27*	117	C4	
			PRR				
2	C	12	YOR346W	*rev1*	107	A11	
2	D	1	YPL167C	*rev3*	108	H11	
2	D	2	YIL139C	*rev7*	142	A10	
2	D	3	YGL087C	*mms2*	126	H11	
2	D	4	YDR092W	*ubc13*	110	E12	
			BER				
2	D	5	YML060W	*ogg1,*	103	A10	
2	D	6	YAL015C	*ntg1*	101	D3	
2	D	7	YOL043C	*ntg2*	107	F12	
2	D	8	YML021C	*ung1*	135	E3	
2	D	9	YER142C	*mag1*	148	G5	
2	D	10	YML028W	*tsa1*	103	C7	
			OTHER				
2	D	11	YMR284W	*hdf1*	104	H11	
2	D	12	YDR227W	*sir4*	121	G7	
2	E	1	YDL042C	*sir2*	146	F3	
2	E	2	YLR442C	*sir3*	145	D6	
2	E	3	YJL092W	*srs2*	133	H8	
2	E	4	YOR005C	*dnl4*	105	G10	
2	E	5	YOL012C	*htz1*	107	E1	

Appendix II. OD_{600} values of growth assay in figure 8